International Journal of Biological Macromolecules 83 (2016) 376–384

Contents lists available at ScienceDirect

International Journal of Biological Macromolecules

journal homepage: www.elsevier.com/locate/ijbiomac

Functional properties of chitosan built nanohydrogel with enhanced glucose-sensitivity

Faheem Ullah, Muhammad Bisyrul Hafi Othman, Fatima Javed, Zulkifli Ahmad, Hazizan Md. Akil*, Siti Zalifah Md Rasib

School of Materials and Mineral Resources Engineering, Engineering Campus, Universiti Sains Malaysia, Seri Ampangan, 14300 Nibong Tebal, Pulau Pinang, Malaysia

ARTICLE INFO

Article history:
Received 8 September 2015
Received in revised form 29 October 2015
Accepted 12 November 2015
Available online 17 November 2015

Keywords:
Nanohydrogel
pH
Glucose sensitivity
Zeta potential
Drug release profile

ABSTRACT

A new approach to design multifunctional chitosan based nanohydrogel with enhanced glucose sensitivity, stability, drug loading and release profile are reported. Two approaches were followed for functionalization of chitosan based nanohydrogel with 3-APBA via EDC and 3-APTES. The effective functionalization, structure and morphology of Chitosan based IPN respectively were confirmed by FTIR, SEM and AFM. At physiological conditions, the glucose-induced volume phase transition and release profile of the model drug Alizarin Red with 1,2-diol structure (comparative to insulin as a drug as well as a dye for bio separation) were studied at various glucose concentrations, pH and ionic strengths. The results suggested a new concept for diabetes treatment and diols sensitivity in view of their potential hi-tech applications in self-regulated on–off response to the treatment (drug delivery and bio separation concurrently).

© 2015 Elsevier B.V. All rights reserved.

1. Introduction

Cell metabolism is the key objective of sensor technology to monitor cell responses to therapeutics and antibiotics. Glucose sensitivity of hydrogel containing glucose-oxidase being a catabolic enzyme with poor stability is reported to reduce the substrate level, hence affecting the cell metabolism [3,11,28]. Thus the ability of PBA (Phenylboronic acid), a synthetic ligand for binding glucose in aqueous medium with better recognition to its counterpart in small volume bioreactors validated its application as moiety in glucose sensor technology. The only problem with PBA is its detection of glucose in alkaline media due to higher pK_a ~8.8 values. Also the existence of charged PBA in tetrahedral state at pH values above the pK_a ~8.8 which bind the diols more readily as compared to uncharged trigonal planar configuration which does not readily complex with cis-diols is a challenge to monitor glucose at physiological conditions. So functionalization of PBA with groups to work at physiological pH is one of the key success for future development [9,19]. Thus incorporation of amino group to PBA leads to work at physiological pH. Infact amine group stabilize the complex formed between PBA and diols. One way of explanation is Lewis acid–base interaction which occurs between electron deficient boron in PBA and electron rich nitrogen in the amine group. Also stronger interaction leads to better solvolysis and much faster time response ($t_{1/2}$ < 5 min) [8,21].

The challenges to find a hydrogel system which would respond only to glucose variations at physiological pH, pharmacokinetics similar to normal pancreatic activity, biocompatibility without any in vivo toxicity and possibly no long term side effect.

Chitosan, the second most abundant natural biopolymer after cellulose, is a linear polysaccharide composed of randomly distributed- (1-4)-linked D-glucosamine and N-acetyl-D-glucosamine units. Actually ionic interactions occur between cationic amino groups of chitosan and negatively charged biomolecules or anion of metals like Pt (II), Pd (II) or Mo (IV) in extreme sensitivity. Also the interchains interaction include H-bonding between ionic molecules and chitosan OH groups or between deacetylated chitosan. Charge density of the small molecules and chitosan is influenced by environmental pH and the material pK_a values [2,4].

The use of (3-dimethylaminopropyl)-3-ethyl carbodimide hydrochloride commonly known as EDC as coupling agent in pharmaceutical formulations which readily hydrolyze and form urea which can be removed from the body by water extraction, is recently employed. We compared its effect with another coupling agent known as 3-aminopropyltriethoxy silane which is the most

* Corresponding author. Tel.: +60 45996161; fax: +60 5941011.
E-mail address: hazizan@usm.my (H.Md. Akil).

http://dx.doi.org/10.1016/j.ijbiomac.2015.11.040
0141-8130/© 2015 Elsevier B.V. All rights reserved.

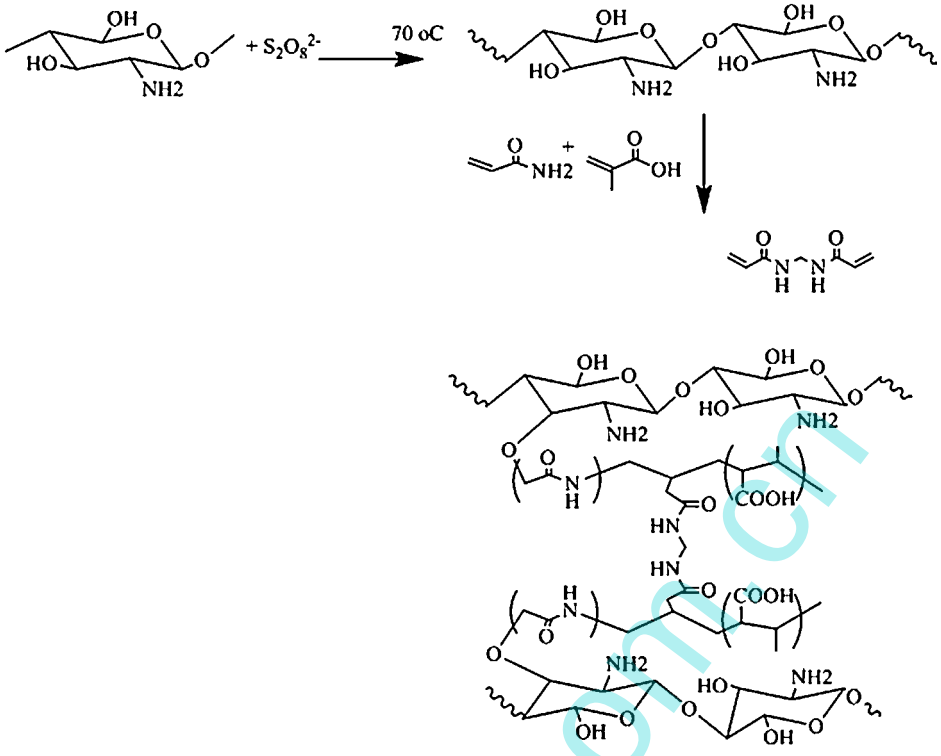

Fig. 1. Proposed mechanism for synthesis of IPN of Chitosan based hydrogels.

used coupling agent in drug delivery systems [16,18]. 3-APTES containing propyl group and a distal amine group for biomolecule attachment. An alkyl salinization is the surface chemistry applied for biosensing, interferometric detection of protein, DNA and also used for the immobilization of bio-molecules for a variety of biomedical applications to build bio-recognition interfaces [17,24]. To compare the properties of both the coupling agents, the effect of surface chemistry-induced charge on the particle uptake was explored in this work. It was observed that due to silane coupling, the PBA were capable of rapidly internalizing with glucose molecules. These finding suggests the finest design of drug delivery vehicles in account to find presentation of glucose molecules.

Fundamental physicochemical and electrokinetic investigations are of utmost importance in order to understand the pH dependency toward glucose sensitivity of the chitosan based nanohydrogel which govern the interaction with the biomolecules (glucose, enzymes, proteins, DNA and dyes). So how and why the changes occur in the hydrogel system with the environment (glucose, pH, ionic strength) depends upon the physical and chemical properties of the system [20,25,30]. Several workers reported the chitosan based hydrogel for drug delivery focusing on the macroscopic films, crosslinkers, microspheres and the reaction conditions but still the effect of internal and external parameters needed to be addressed. Our efforts showed enhanced results with desirable properties by introducing a new coupling agent into such systems, which tuned the internal and external properties. The investigation of physicochemical, electrokinetic parameters with a model drug loading Vs release profile simultaneously by the new coupling agent may attracts the scientist for future drug delivery with pre-determined physical and chemical properties.

Chitosan-poly (acrylamide-co-methacrylic acid) IPNs were prepared by free radical co-polymerization using methylenebisacrylamide and ammonium peroxysulphate as crosslinker and initiator respectively. The effect of pH, glucose and ionic strength on physicochemical and electrokinetic investigations in terms of swelling, zeta potential, conductance and electrophoric mobility were studied in detail. The model drug Alizarin Red (comparative to insulin as a drug as well as a dye for bio separation) was used to study the loading and release profile for the hydrogel in terms of absorbance by using UV–vis-Spectroscopy. Consequently the pronounced effect of 3-APTES coupling was determined with enhanced sensitivity toward diols.

2. Experimental

2.1. Materials

Chitosan ($M_w \approx 160{,}000$ g/mol, degree of deacetylation DD ≈ 90%) N,N-methylenebisacrylamide (MBA) were obtained from Acros (Geel, Belgium), while all other chemicals were purchased from Aldrich (St. Louis, MO, USA). Methacrylic acid (MAA) which was purified by distillation at reduced pressure to remove hydroquinone inhibitor. 3-aminophenylboronic acid (3-APBA), N-ethyl-carbodimide hydrochloride (EDC), D(+)-Glucose, 3-aminopropyltriethoxy silane (3-APTES) and all buffer solutions were used as received without purification. Deionized distilled water (DDH_2O) followed by filtration through a 0.2 μm filter to remove any dust was used for all solution preparation, polymerization, dialysis and analysis steps.

2.2. Synthesis of chitosan-poly (acrylamide-co-methacrylic acid) hydrogel

Chitosan-poly (acrylamide-co-methacrylic acid) hydrogels were synthesized by free radical co-polymerization. Initially chitosan (500 mg) was dissolved in 80 mL (DDH_2O + 0.35 mL acetic acid) with constant stirring for 06 h at room temperature, followed by the addition of AAm, MAA in a three neck round bottom flask equipped with N_2 inlet and condenser with constant stirring for 10 h at room temperature. After 16 h stirring under N_2 purging at room temperature the crosslinker (MBA dissolved in 10 mL of DDH_2O was added to the solution drop-wise and temperature was

Table 1
Feed composition of p(Chitosan-co-AAm-co-MAA) nanohydrogel particles.

Sample code	3-APBA (mg)	EDC (mg)	3-APTES (mg)	Curing time (h)	Curing temp. (°C)	Dialysis (days)
A	–	–	–	18	70	05
A1	115	115	–	28	25	07
A2	115	–	115	28	25	07

raised gently at the rate of 1 °C/min to 70 °C. After 01 h of achieving the desired temperature 10 mL of initiator (0.05 M) were added drop-wise to the reaction mixture to start the polymerization and continued for 01 h at 70 °C under constant stirring and N_2 purging as shown in Fig. 1. Several minutes after the addition of APS the reaction mixture turned milky. The resultant hydrogels were then purified by centrifugation, decantation followed by washing with DDH_2O. Finally the hydrogels were purified at room temperature by dialysis for 05 days in membrane tubing (Spectrum laboratories, Inc., Rancho Dominguez, CA, USA; cutoff 12,000–14,000).

2.3. Functionalization of chitosan-poly (acrylamide-co-methacrylic acid) by 3-APBA

Chitosan-poly (acrylamide-co-methacrylic acid) were successfully functionalized with 3-APBA by dissolving 0.115 g of EDC and 0.115 g of 3-APBA in 60 mL DDH_2O respectively with continuous stirring for 04 h at room temperature as shown in Table 1. The solution was then placed in an ice bath followed by addition of 20 mL of dialyzed hydrogel under continuous stirring for 06 h and again purified by dialysis for 07 days with frequently changing water after every 12 h. Similar scheme was followed for functionalization of the hydrogel by 3-APBA via 3-APTES catalyzed coupling of 3-APBA to –OH groups in methacrylic acid units as shown in Fig. 2.

2.4. Characterization

The FTIR spectra of the over dried hydrogel samples coded as A, A1 and A2 were recorded using (Waltman, MA, USA) Spectrum for the identification of different functional groups present in the systems in 4000–400 cm^{-1} range. Before measuring Zeta potential with the help of nano-zetasizer (Malvern Instruments, Malvern, UK using He-Ne Laser with 633 nm wavelength and a detector angle of 173°), the pH of all the solutions was measured using (Weilheim, Germany) inoLab pH 720 pH meter. All solutions were prepared in the desired buffer as per experimental requirements. It should be noted that each reported value is the average of three measurements taken in the cylindrical cell at stationary level. The standard deviation, every time was less than 4% (Tables 2–4).

A similar approach was followed to find the particle size using dynamic laser light scattering (DLS) measurements by using NANO ZS Zetasizer with a He–Ne Laser working at 633 nm wavelength and a detector angle of 90°. Before each reading, each solution was passed through Millipore Millex-HV filter (pore size ≈ 0.20 μm) in order to remove any entrapped dust particles. The required

Table 2
FTIR spectroscopy absorption bands of Chitosan based functionalized hydrogels.

Possible assignment	Frequency (cm^{-1})
H-bonded O–H groups	3650
N–H	1660
C–H	1350.5
C=O	1760
C–O	1133.5
Phenyl	666–995
NH_2 stretching	1590

Table 3
Summary of physicochemical parameters at physiological environs.

Physiological conditions	Sample code	*z*-average (nm)	*z*-potential (mv)
pH 7.45	A1	241	−12.14
	A2	270	−7.18
Glucose conc. (120 Mm)	A1	259	−18.55
	A2	402	−22.33
Ionic strength (0.5 M NaCl)	A1	190	−27.32
	A2	149	−30.50

Table 4
Summary of electrokinetic parameters at physiological environs.

pH 7.45		Conductance (mv)	Ionic mobility
	A1	25.5	−0.67
	A2	31.9	−0.45
Glucose conc. (120 Mm)	A1	16.3	−1.12
	A2	24.6	−1.42
Ionic strength (0.5 M NaCl)	A1	14.2	−0.95
	A2	17.8	−1.06

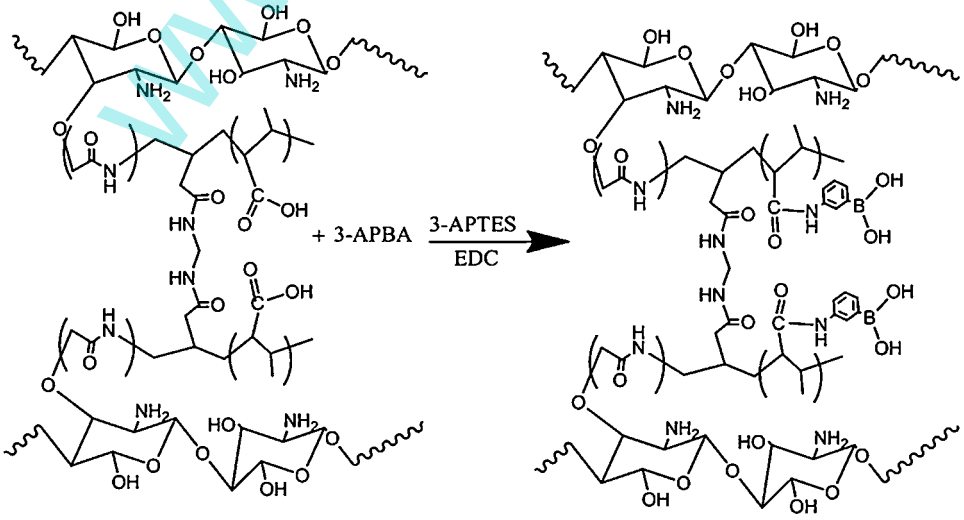

Fig. 2. Functionalization of nanohydrogel with 3-APBA toward glucose sensitivity.

www.spm.com.cn

solutions were first equilibrated for 20 min before every reading with three times repetition. The correlation functions were analyzed by the constrained regularized CONTIN method to obtain distribution decay rates (s). The decay rates gave the distribution of the apparent mutual diffusion coefficient $D_{app} = \Gamma/q^2$ with the scattering vector (Eq. (1) [27].

$$q = \left(\frac{4\pi n}{\lambda}\right) \sin\left(\frac{\theta}{2}\right) \quad (1)$$

where n is the refractive index of water. The hydrodynamic diameter, D_h can be calculated by using the Stokes–Einstein equation (Eq. (2)) [27].

$$D_{h,app} = \frac{kT}{3\pi\eta D_{app}} \quad (2)$$

where k is the Boltzmann constant, η is the viscosity of water at absolute temperature T and $D_{h,app}$ is the apparent hydrodynamic diameter of equivalent hard sphere. For all pH range (1.68–12.45), glucose concentration (0.1–300 mM) and ionic strength (0.1–3.0 M) the scattering intensities were measured. The correlation functions obtained from DLS were then analyzed to get distribution decay rates, hydrodynamic diameter and viscosities. Alizarin red (ARS), a dye with 1,2-diol structure, was selected as a model drug (comparative to insulin) to study the loading and release absorbance profile for both type of hydrogels by UV–vis spectrophotometer.

3. Results and discussion

3.1. Structure confirmation

Our approach to prepare glucose sensitive nanohydrogel involve first the preparation of chitosan-poly (acrylamide-co-methacrylic acid) hydrogel by free radical co-polymerization followed by functionalization of the hydrogel with 3-APBA as glucose sensing moiety. It was observed that incorporation of acrylamide leads to the stability of the hydrogel over a wide range of pH and glucose concentrations as it acts as a ligand and also a future perspective for further studies in the field of optical sensing in presence and absence of metallic nanoparticles in biosensors.

The chemical structures of chitosan-poly (acrylamide-co-methacrylic acid) and after functionalization of carboxyl group by 3-APBA using EDC and 3-APTES coupling agents were confirmed by FTIR spectroscopy as shown in Fig. 3.

The characteristic absorption peaks of chitosan at 1660–1570 cm^{-1} can be assigned to amine stretching (amide bands) and carbonyl stretching of aminoacetyl group of chitosan. The C–H stretching of chitosan is clear at 1350.5 cm^{-1} while representative peaks at 900 cm^{-1}, 1160 cm^{-1} and 1570 cm^{-1} correspond to saccharide structure of chitosan. The broad peaks appears at 1760–1700 cm^{-1} correspond to C=O stretching vibrations [5,14]. The C–N stretching in the amine group appears at 1250–1340 cm^{-1}. It is clear from the figure that the peak at 1133.5 cm^{-1} which is due to C–O stretching vibration in chitosan spectrum is shifted exactly at 1169.5 cm^{-1} in both cases (b and c) due to functionalization of the system. Furthermore, the most successful functionalization of 3-APBA containing –OH groups appear very accurately at 3650–3590 cm^{-1}. A strong look for phenyl stretching occurs at 666 cm^{-1} and 985 cm^{-1} which is also a justification of successful functionalization of the system. Shifting in the positions of peaks as compared to pure hydrogel system represent the functionalization of the system by 3-APBA.

3.2. Morphology

Scanning electron microscope (SEM-JEOL JSM6360LV, JAPAN) was used to determine the morphologies of nanohydrogel particles and aggregates. The bright spots representing very small conductance as determined from Zeta nanosizer because the samples were scanned without coating for SEM analysis. The gel samples were placed on an aluminum mount, sputtered with gold and palladium and then scanned at an accelerating voltage of 5.0 kV as shown in Fig. 4.

AFM images were recorded on a Benyuan CSPM 5500 Scanning Probe Microscope in tapping mode under ambient conditions. The drug loaded image of A2-modified via 3-APTES were composed of a much larger grain size (220 nm) as compared to unloaded A2 (100 nm). To evaluate the surface profile of A2, one of the most general and most useful roughness parameters, root mean square (RMS) roughness was applied. The calculated equilibrium RMS roughness of the loaded and unloaded A2 was observed to be 9.43 nm and 100 nm. The decrease in RMS roughness of loaded A2 may be explained by the disordered attachment of the drug to 3-APBA moieties as shown in Fig. 5.

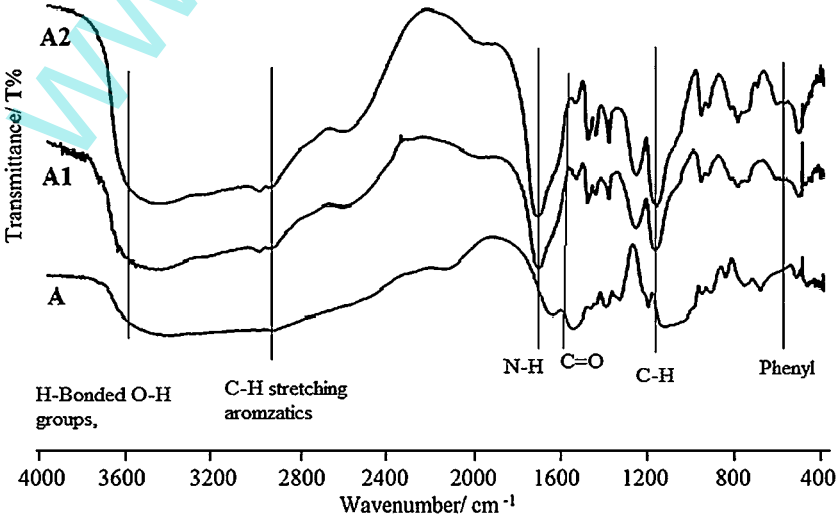

Fig. 3. Representative FTIR spectra of Chitosan based hydrogels.

www.scm.com.cn

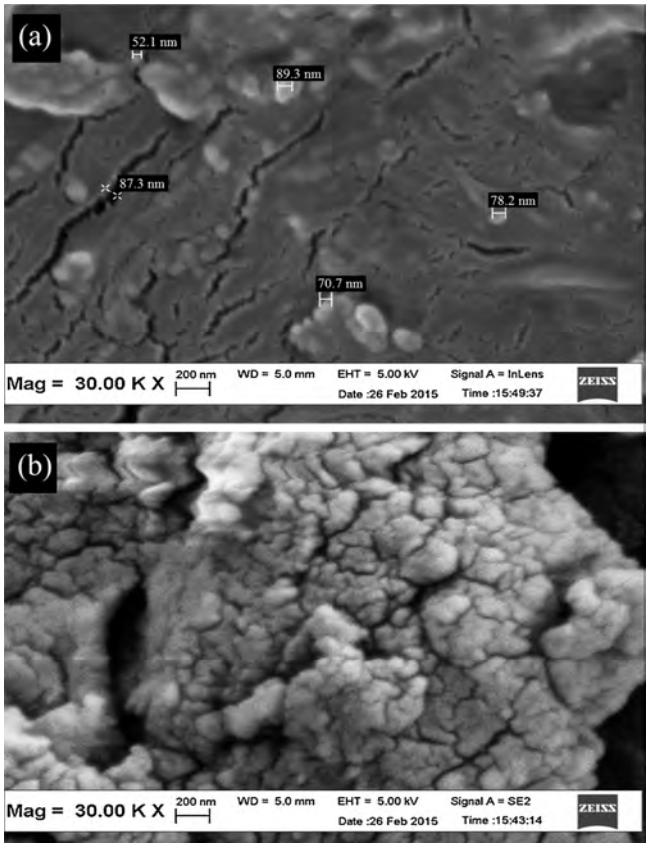

Fig. 4. SEM images of unloaded A2 (a), loaded A2 (b) with ARS at pH 7.45 and $T = 25\,^{\circ}C$.

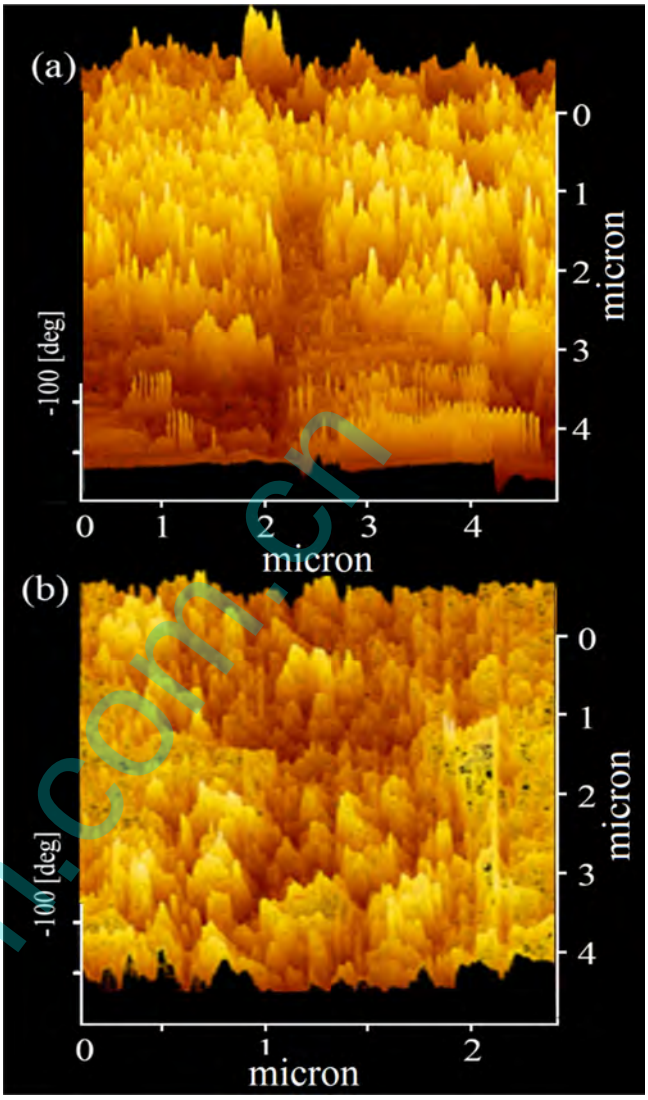

Fig. 5. AFM images of unloaded A2 (a), loaded A2 (b) with ARS, at pH 7.45 and $T = 25\,^{\circ}C$.

3.3. Physicochemical investigations

3.3.1. pH effect

In order to see the effect of pH on the average calculated values of hydrodynamic diameter (*z*-average) and Zeta potential, we plotted these values as a function of pH as shown in Fig. 6.

Actually the swelling of hydrogels containing pH responsive moieties is controlled by the internal osmotic pressure that arises due to motions of the ions and its counter ions. Also this ion–counter ion interaction has a role to balance the electrostatic repulsion. It is clear from the graph that at lower pH the COO^- groups are protonated to COOH due to which the hydrogel is present in shrunken state with less hydrodynamic size [7,26]. It was observed that at low pH the shrunken of hydrogel occur as the COOH groups reduces the columbic repulsion that occur among the hydrogel particles and also responsible for the increased H-bonding between chitosan and other chains. Another argument to explain the shrinkage of the hydrogel at lower pH is in the light of pK_a and degree of ionization. When pH value reaches the pK_a value of chitosan ($pK_a \approx 6.5$), the NH_2 groups slightly become protonated but PMAA have ($pK_a \approx 5.5$) needed lower pH for the protonation of all its COO^- groups. Consequently positively charged $^+NH_3$ groups of chitosan and some negatively charged COO^- groups of PMAA due to electrostatic interaction results in the reduction of size of the hydrogel. It is important to mention here from the discussion that both chitosan and PMAA are pH sensitive. The graph also shows that by increasing the pH, the particle size increases sharply up to pH 7.45 (physiological pH) but further increased in size is also shown at higher pH which is attributed to higher degree of ionization of the respective groups.

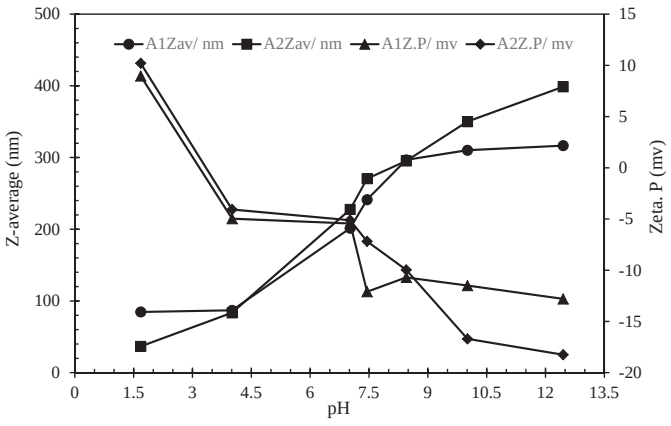

Fig. 6. The plot of hydrodynamic diameter (*z*-average) and Zeta potential as a function of pH (1.68–12.45) at $25\,^{\circ}C$.

www.spm.com.cn

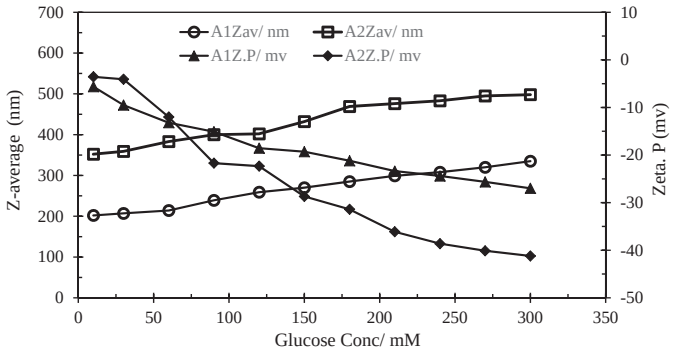

Fig. 7. Plot of hydrodynamic diameter (*z*-average) and Zeta potential as a function of glucose concentration (0.1–300 mM).

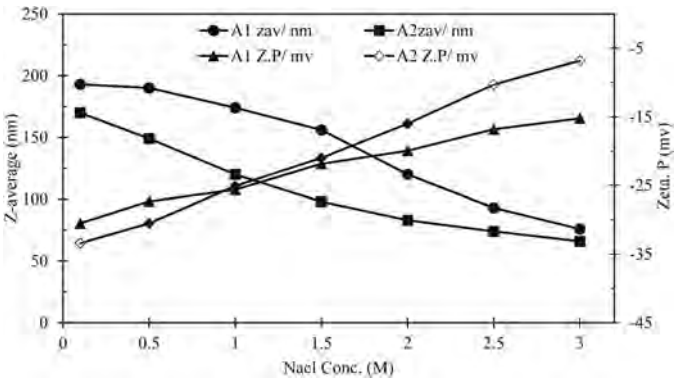

Fig. 8. Plot of hydrodynamic diameter (*z*-average) and Zeta potential as a function of (0.1–3 M NaCl).

3.3.2. Glucose effect

The most important is the functionalization of hydrogel by incorporation of 3-APBA using different coupling agents (EDC and 3-APTES). Our strategy to enhance the glucose sensitivity is the main objective of this work. The incorporation of 3-APBA make the hydrogel glucose sensitive. Earlier work focused only on the sensitivity of higher or lower glucose concentration, but we further developed the new method to enhance the glucose sensitivity both at higher and lower concentrations with their physicochemical and electro-kinetic investigations at physiological conditions. With increase in glucose concentration the particle size expand dramatically. The particle size increases from 202 nm to 285 for A1 and from 352 to 469 for A2 by increasing glucose concentration as clear from the Fig. 7.

This property is attributed to the stabilization of charged phenylborate by complexation with glucose which is believed to convert more hydrophobic uncharged groups of 3-APBA to hydrophilic charged 3-APBA groups at pH 7.45. As our samples are not temperature sensitive but an effort was made to study the temperature response on the volume changes. As compared to higher temperatures (up to 70 °C the significant swelling was observed at 30–40 °C which also confirmed the desired nature of our hydrogel system working at physiological temperature, but the temperature dependent profile was not included in the this section. Again the pH effect is more pronounced on the glucose sensitivity of the functionalized hydrogels. As stated earlier at lower pH the PBA groups were in uncharged form so the systems lose their response to glucose sensitivity but at higher pH, due to ionization of 3-APBA groups, the response to glucose sensitivity originated where one can differentiate the swelling ratio at lower and higher pH values.

3.3.3. Ionic strength effect

In the proceeding section, the effect of ionic strength is described which has a marked effect on the glucose sensitivity of the hydrogel systems. From the Fig. 8, it is clear that increasing ionic strength, the swelling response of the hydrogel decreases.

This effect can be explained by the weakening of Donnan potential. At very low concentration of NaCl (0.05 mol L^{-1}), the swelling is more pronounced as compared to higher ionic strength, representing the desired system can work at the physiological ionic strength (blood ionic strength). The higher ionic strength may leads to change the viscosity of the system (salt–glucose–water system) due to vitrification [22,29] which decreases the concentration of glucose and thus reduces the particle size.

Furthermore increasing NaCl concentration leads to decrease in size of the nanohydrogel particles, which may be related to the lessening of the repulsive potential that results in increase of precipitation or flocculation [10].

3.4. Electrokinetic investigations

3.4.1. Zeta potential

Zeta potential is the key parameter that controls the electrostatic interactions in particle dispersion and hence the stability. Actually the distribution of ions in the surrounding interfacial region is affected by the charge at the particle surface and increased concentration of counter ions close to the surface which result in electrical double layer formation. When the particle moves, ions within the boundary also move with it, thus the ions beyond the boundary stay with the bulk dispersant. The potential at this boundary is called the Zeta potential [12,13]. The positive values of Z.P is due to increase in number of positively charged $^{+}NH_3$ groups on the chitosan chains. Due to excess $^{+}NH_3$ groups in the medium at low pH there rises a Donnan potential for the hydrogel system which results in some degree of repulsion. Apart from these, other interaction such as hydrophobic interaction, association of methylene groups of MBA, amine groups of AAm and chitosan chains also have a key role in creating the charge and hence Z.P. Furthermore as the pH increases, the positively $^{+}NH_3$ groups of chitosan and AAm chains are balanced by negative chains of 3-APBA which results in the interaction and causes the swelling of hydrogels. Zeta potential measured as a function of pH, glucose concentration and ionic strength is shown in the Figs. 6–8. It is clear that at lower pH, the values of Z.P are positive and becomes negative with increasing pH. The zero value of Z.P represents the isoelectric point where positively charged groups on chitosan are balanced by the negatively charged groups on PBA groups. It is normally the point where the colloidal system is least stable. As the pH increases, the values of Z.P become negative, this is attributed to higher degree of ionization of the negative groups of the system. At further increased pH, the negative values of Z.P became constant showing maximum ionization of the negative groups present in the system. It is clear from the discussion that Z.P measurement not only gives the quantitative and qualitative information about the charge on the overall particle but also explores the stability for drug loading and release profile at physiological environments.

3.5. Electrophoric mobility and electrokinetic phenomena

In order to find the relation of Z.P (ζ) to electrophoric mobility (μ) we consider the Eq. (3) [15].

$$\xi = \frac{3\eta\mu X 1}{2\varepsilon o\varepsilon r.f} \tag{3}$$

According to the equation Z.P is directly related to the electrophoric mobility of the nanohydrogel particles. It is not too simple to say that higher the values of electrophoric mobility, higher will be the Z.P, as practically there are contributions of frictional forces

www.spm.com.cn

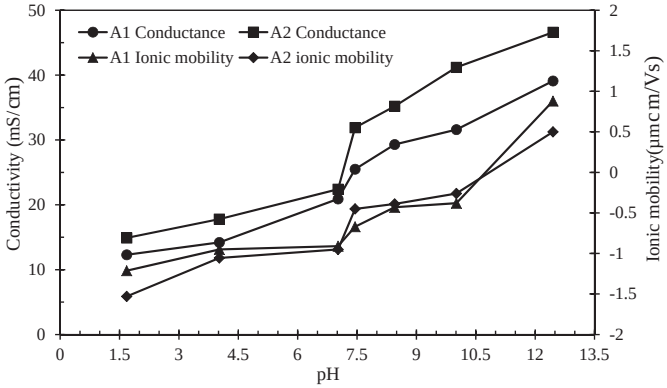

Fig. 9. Dependence of conductance and ionic mobility on the on pH (1.68–12.45) at 25 °C for A1 and A2 in aqueous solutions.

and the charge density to the overall Z.P. This was observed that higher the swelling at higher charge density as compared to lower charge density due to higher friction during the motion of particles. So another contribution from friction of the moving particles, ion condensation from condensed charged system, diffusional motion and electrostatic balance of the ions all leads to the onset of Z.P. So the change in Z.P as a function of glucose concentration and pH is due to variations in number of positive and negative groups in the overall hydrogel system. Consequently increasing the pH, the surface charge density of the particles increases leads to increase in the electrophoric mobility and thus the conductance as shown in Figs. 9 and 10.

From our conclusions we established that electrophoresis can help to create a difference between dilute and concentrated solutions by reviewing the dependence of the electrophoretic mobility on the concentration of dispersed particles. If there is no dependence, the behavior is that of a dilute system for which there is a direct relation observed in case of pH, glucose and ionic strength.

3.6. Surface conductivity and electrokinetic phenomena

Surface conduction is the name given to the excess electric conduction that takes place in dispersed systems owing to the presence of the electric double layers. Excess charges in them may move under the influence of electric fields applied tangentially to the surface. The phenomenon is quantified in terms of the *surface conductivity*, which is the surface equivalent to the bulk conductivity, σ is a surface excess quantity just as the surface concentration, the electrical conductivity σ of an aqueous solution of polyelectrolytes originated by the movement of any charged entity in response to an external applied electric field, depends on three independent

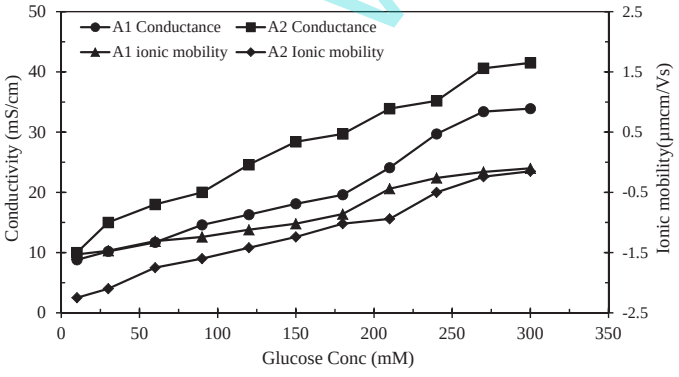

Fig. 10. Dependence of conductance and ionic mobility on the on glucose conc. (0.1–300 mM) at 25 °C for A1 and A2 in aqueous solutions.

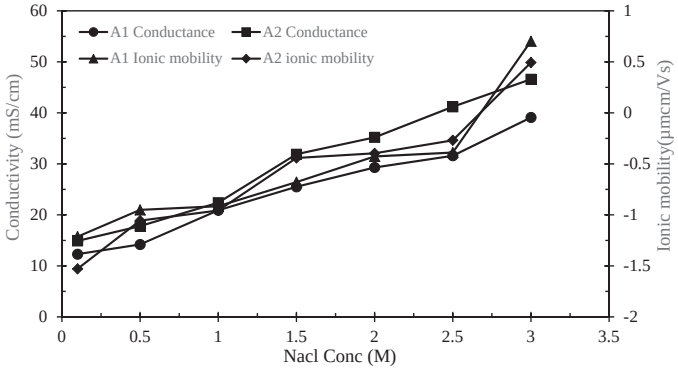

Fig. 11. Dependence of conductance and ionic mobility on the ionic strength (0.1–3 M NaCl) at 25 °C for A1 and A2 in aqueous solutions.

contributions, i.e., the numerical concentration n_i of the charge carriers of type i, their electrical charge ($Z_i \cdot e$) and their ionic mobility μ_i, according to the relationship (Eq. (4)) [1]

$$\sigma = \Sigma i (Z_i \cdot e) n_i \mu_i \quad (4)$$

Here, the mobility μ is defined as the ratio of the average velocity of the charged carrier to an applied electric field of unit strength. Eq. (4) can be written in a more usual way if we express the numeric concentration n_i through the molar concentration C_i ($n_i = N_A \cdot C_i$, where N_A is the Avogadro number) and the mobility μ_i through the equivalent conductance λ_i ($\mu_i = \lambda_i / F$, where $F = e \cdot N_A$ is the Faraday constant). So the Eq. (4) becomes Eq. (5).

$$\sigma = \Sigma i (Z_i) C_i \lambda_i \quad (5)$$

From the Eq. (4) and Eq. (5), it is clear that increasing that the numeral concentration, has a direct effect on the ionic mobility and thus the conductance as clear from the Figs. 10 and 11.

3.7. Photoluminescence investigations

A number of mechanism are explored by workers for drug loading by diffusion, entrapment and tethering but the selection of method depends on the nature of the system [6,23]. Our strategy is to study the loading and release profile of the drug by diffusion into the hydrogel system due to its porous and compatible nature for the model drug. Pre-weighed samples of both the hydrogels A1 and A2 were placed separately in equimolar Alizarin red solutions. First the diffusion of the drug in terms of absorbance was measured after every 30 min until maximum loading was observed. Similarly after complete loading, the release profile was also investigated for both the hydrogels by immersing the loaded-dried hydrogel in glucose solutions of known concentration. It is important to discuss here that local drug release by diffusion provides a basic mechanism for non-specific drug release, but biological and chemical triggers offer a very finer tuned control for selective treatment. Moreover release triggers also moderate the speed of drug release to maintain effective drug levels at the local site of action without raising exposure to toxic levels. Inside the body the factors responsible for the variability in the efficacy of treatment are the extreme acidic pH and higher enzymatic activity that's why the choice of selection needs specific groups that responds to the desired conditions.

3.8. Drug loading profile

Alizarin Red with 1,2-diol structure comparative to Insulin as a drug as well as a dye for bioseparation purpose was selected to study the multifunctional behavior of the chitosan based nanohydrogel. Both the hydrogels were immersed in ARS solutions and the loading of ARS was traced by UV–vis spectra. A quick loading

www.spm.com.cn

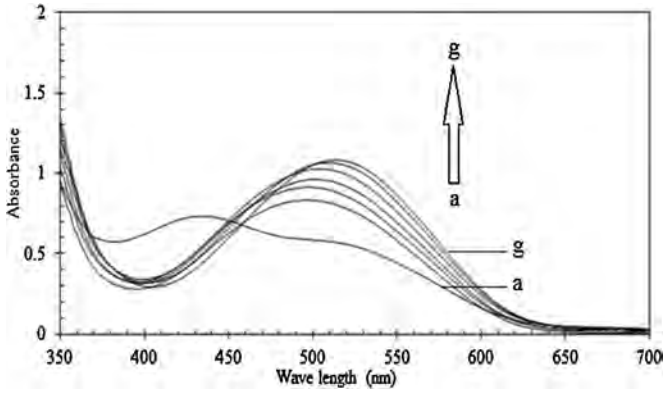

Fig. 12. Absorption spectra of A1 loaded with ARS from ARS/PBS (pH 7.4) medium at 431 nm.

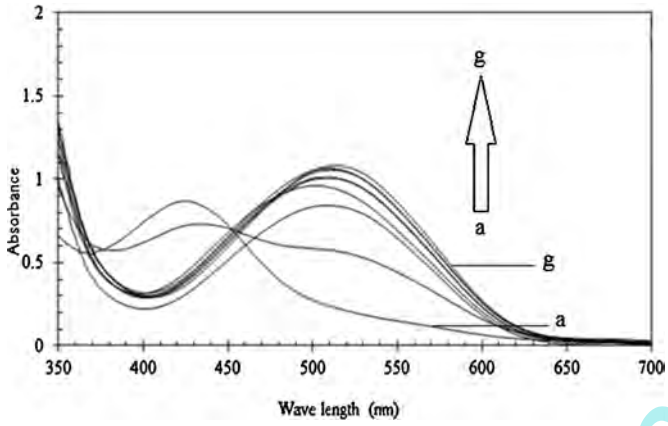

Fig. 13. Absorption spectra of A2 loaded with ARS from ARS/PBS (pH 7.4) medium at 431 nm.

was observed at first and slowed down gradually followed by equilibrium loading in 450 min. The absorption bands of ARS shifted from 431 nm to 512 nm in both the samples which is the indication of complexation of PBA with the model drug Alizarin red. For comparison the spectra of both the loaded hydrogels are shown in Figs. 12 and 13 respectively.

3.9. Drug release profile

The initial quick release followed by gradual release was observed for both the nanohydrogel in a pre-determined glucose solution as clear from Figs. 14 and 15. The release of the model drug

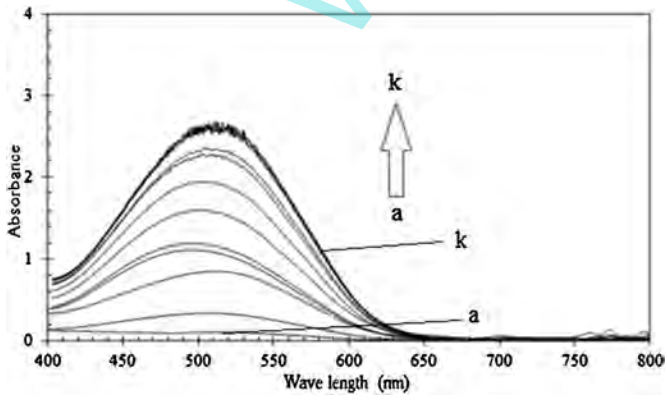

Fig. 14. Release spectra of ARS from A1 in glucose/PBS (pH 7.4) medium at 520 nm.

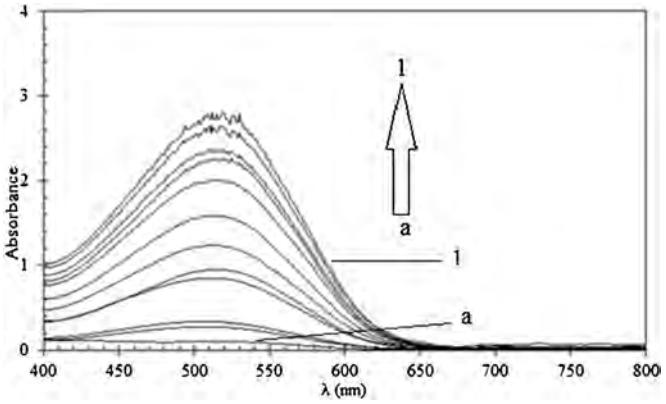

Fig. 15. Release spectra of ARS from A1 and A2 in glucose/PBS (pH 7.4) medium at 520 nm.

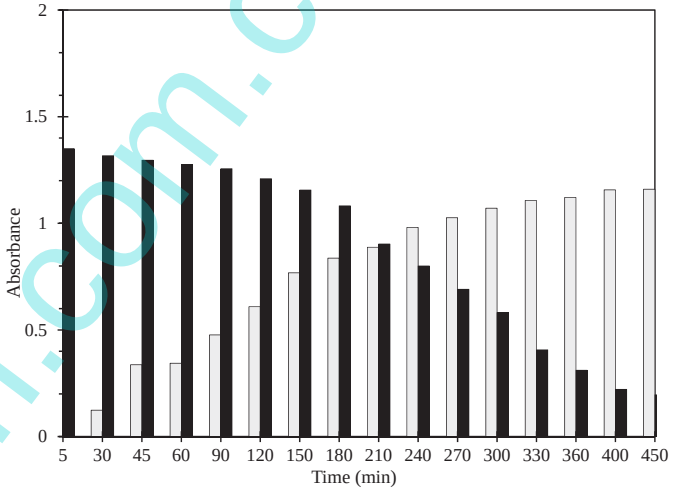

Fig. 16. Loading and release profile of ARS from ARS/PBS solution showing equilibrium loading of ARS in the system.

was suggested as a process to re-establish the equilibrium among the bound Alizarin red to 3-APBA, free Alizarin red and free 3-APBA groups in the systems. The competition of glucose with the model drug for 3-APBA binding sites is clear from the graphical abstract which is the basis of enhanced glucose sensitivity if the selected system (Fig. 16).

A close examination of both the profile reveal that the release of Alizarin red in pure Glucose/PBS (pH 7.45) solution decreased uniformly with the passage of time. It showed the uniform replacement of ARS by glucose and also the compatible nature of the system to glucose. These results confirm that the release of Alizarin is mainly controlled by the replacement of Alizarin by glucose at each instance giving another successful path to our targeted work.

4. Conclusion

IPN of chitosan based nanohydrogel prepared by free radical co-polymerization method were successfully functionalized with 3-APBA, a glucose sensing moiety via EDC and 3-APTES coupling agents respectively. The effects of coupling agents and functionalization with glucose sensing moiety on the physicochemical and electrokinetic parameters showed pH and saccharide sensitive behaviors. Alizarin red as a model drug to study the loading and release profile showed that the release was faster in the presence of glucose which competes with the drug for binding sites. We believe that bioseparation of dyes containing diols structures and

www.scpm.com.cn

especially the drug glycosylated insulin may bind to and release from the nanohydrogel systems in a similar way as Alizarin red. Consequently the novel multifunctional chitosan based nanohydrogel may find applications in bioseparation and self-regulated insulin delivery with enhanced sensitivity toward glucose.

Acknowledgments

This research is supported by the School of Material and Mineral Source Engineering, Universiti Sains Malaysia under the project Grant FRGS-203/PBAHAN/6071242. The author is highly grateful to The World Academy of Sciences (TWAS, for the advancement of science in developing countries) and USM for a TWAS-USM Ph.D. fellowship.

References

[1] A. Stuart, H. Wu, U. Twahir, H. Pei, Conductivity and electrophoretic mobility of dilute ionic solutions, J. Colloid Interface Sci. 352 (2010) 1–10.
[2] B. Jérôme, M. Reist, J.M. Mayer, N.A. Olivia Felt, P.R. Gurny, 'Structure and interactions in covalently and ionically crosslinked chitosan hydrogels for biomedical applications', Eur. J. Pharm. Biopharma. 57 (2004) 19–34.
[3] K. Chaturvedi, K. Ganguly, M.N. Nadagouda, T.M. Aminabhavi, Polymeric hydrogels for oral insulin delivery, J. Control. Release 165 (2013) 129–138.
[4] D. Laurent, T. Vincent, A. Domard, E. Guibal, Preparation of chitosan Gel beads by ionotropic molybdate gelation, Biomacromolecules 2 (2001) 1198–1205.
[5] D. Caixia, L. Zhao, F. Liu, J. Cheng, J. Gu, S. Dan, C. Liu, X. Qu, Z. Yang, Dually responsive injectable hydrogel prepared by in situ cross-linking of glycol chitosan and benzaldehyde-capped peo-ppo-peo, Biomacromolecules 11 (2010) 1043–1051.
[6] D. Sanjeev, A Chitosan-Polymer Hydrogel Bead System for a Metformin Hci Controlled Release Oral Dosage Form, 2011.
[7] A. Döring, W. Birnbaum, D. Kuckling, Responsive hydrogels – structurally and dimensionally optimized smart frameworks for applications in catalysis, micro-system technology and material science, Chem. Soc. Rev. 42 (2013) 7391–7420.
[8] E. Yuya, R. Miki, T. Seki, Colorimetric sugar sensing using boronic acid-substituted azobenzenes, Materials 7 (2014) 1201–1220.
[9] Z.H. Farooqi, W. Wu, S. Zhou, M. Zhou, Engineering of phenylboronic acid based glucose-sensitive microgels with 4-vinylpyridine for working at physiological ph and temperature, Macromol. Chem. Phys. 212 (2011) 1510–1514.
[10] G. Maria, K. Szczubiałka, B. Wowra, D. Dobrowolski, B. Orzechowska-Wylęgała, E. Wylęgała, M. Nowakowska, Hydrogel membranes based on genipin-cross-linked chitosan blends for corneal epithelium tissue engineering, J. Mater. Sci. Mater. Med. 23 (2012) 1991–2000.
[11] G. Zhen, T.T. Dang, M. Ma, B.C. Tang, H. Cheng, S. Jiang, Y. Dong, Y. Zhang, D.G. Anderson, Glucose-responsive microgels integrated with enzyme nanocapsules for closed-loop insulin delivery, ACS nano 7 (2013) 6758–6766.
[12] J. Barbara, M. Wasilewska, Z. Adamczyk, Characterization of globular protein solutions by dynamic light scattering, electrophoretic mobility, and viscosity measurements, Langmuir 24 (2008) 6866–6872.
[13] K. Michael, J. Corbett, F.M. Watson, A. Jones, High-concentration Zeta potential measurements using light-scattering techniques, Philos. Trans. R. Soc. Lond. A: Math. Phys. Eng. Sci. 368 (2010) 4439–4451.
[14] K. Abbas, M.B.H Othman, K. Abdul Razak, H. Md Akil, Synthesis and physicochemical investigation of chitosan-Pmaa-based dual-responsive hydrogels, J. Polym. Res. 20 (2013) 1–8.
[15] K. Shanza Rauf, Z.H. Farooqi, M. Ajmal, M. Siddiq, A. Khan, Synthesis, characterization, and silver nanoparticles fabrication in N-isopropylacrylamide-based polymer microgels for rapid degradation of P-nitrophenol, J. Dispers. Sci. Technol. 34 (2013) 1324–1333.
[16] L. Mikael, W-C. Huang, M-H. Hsiao, Y-J. Wang, M. Nydén, S-H. Chiou, D-M. Liu, Biomedical applications and colloidal properties of amphiphilically modified chitosan hybrids, Prog. Polym. Sci. 38 (2013) 1307–1328.
[17] L. Chang-Soo, S.K. Kim, M. Kim, Ion-sensitive field-effect transistor for biological sensing, Sensors 9 (2009) 7111–7131.
[18] Li. Chenghong, G.L. Wilkes, The mechanism for 3-aminopropyltriethoxysilane to strengthen the interface of polycarbonate substrates with hybrid organic–inorganic sol-gel coatings, J. Inorg. Organometall. Polym. 7 (1997) 203–216.
[19] L. Pengxiao, Q. Luo, Y. Guan, Y. Zhang, Drug release kinetics from monolayer films of glucose-sensitive microgel, Polymer 51 (2010) 2668–2675.
[20] G.A. Morris, S.M. Kök, S.E. Harding, G.G. Adams, Polysaccharide drug delivery systems based on pectin and chitosan, Biotechnol. Genet. Eng. Rev. 27 (2010) 257–284.
[21] P. Brighid, M.J. Kiefel, T.A. Houston, Boron-Carbohydrate Interactions, INTECH Open Access Publisher, 2012.
[22] Q. Yong, K. Park, Environment-sensitive hydrogels for drug delivery, Adv. Drug Deliv. Rev. 64 (2012) 49–60.
[23] V. Ravaine, C. Ancla, B. Catargi, Chemically controlled closed-loop insulin delivery, J. Controlled Release 132 (2008) 2–11.
[24] S. Beniamino, E. Secret, S. Pace, P. Gonzalez, F. Geobaldo, F. Quignard, F. Cunin, Chitosan-functionalized porous silicon optical transducer for the detection of carboxylic acid-containing drugs in water, J. Mater. Chem. 21 (2011) 2294–2302.
[25] S.K. Shukla, A.K. Mishra, O.A. Arotiba, B.B. Mamba, Chitosan-based nanomaterials: a state-of-the-art review, Int. J. Biol. Macromol. 59 (2013) 46–58.
[26] A.C.S. Martien, W.T.S. Huck, J. Genzer, M. Müller, C. Ober, M. Stamm, G.B. Sukhorukov, I. Szleifer, V.V. Tsukruk, M. Urban, Emerging applications of stimuli-responsive polymer materials, Nat. Mater. 9 (2010) 101–113.
[27] U. Faheem, A. Khan, H. Md Akil, M. Siddiq, Effect of hydrophilic/hydrophobic block ratio and temperature on the surface and associative properties of oxyethylene and oxybutylene diblock copolymers in aqueous media, J. Dispers. Sci. Technol. 36 (2015) 1777–1785.
[28] W. Zhongming, S. Zhang, X. Zhang, S. Shu, T. Chu, D. Yu, 'Phenylboronic acid grafted chitosan as a glucose-sensitive vehicle for controlled insulin release', J. Pharma. Sci. 100 (2011) 2278–2286.
[29] Z. Rhongsheng, M. Tang, A. Bowyer, R. Eisenthal, J. Hubble, A novel Ph-and ionic-strength-sensitive carboxy methyl dextran hydrogel, Biomaterials 26 (2005) 4677–4683.
[30] Z. Wenbo, Yi. Fang, Q. Zhu, K. Wang, M. Liu, X. Huang, J. Shen, A novel glucose biosensor based on phosphonic acid-functionalized silica nanoparticles for sensitive detection of glucose in real samples, Electrochim. Acta 89 (2013) 278–283.

www.spm.com.cn